Chemical Engineering Journal 144 (2008) 299–311

Contents lists available at ScienceDirect

Chemical Engineering Journal

journal homepage: www.elsevier.com/locate/cej

Pressure drop modeling on SOLID foam: State-of-the art correlation

David Edouard [a,*], Maxime Lacroix [a], Cuong Pham Huu [a], Francis Luck [b]

[a] LMSPC, UMR 7515 CNRS, ECPM, Université Louis Pasteur-ELCASS, 25 rue Becquerel 67087 Strasbourg, France
[b] TOTAL S.A., Direction Scientifique, 2 place de la Coupole 92078 Paris La Défense Cedex, France

ARTICLE INFO

Article history:
Received 28 February 2008
Received in revised form 6 June 2008
Accepted 10 June 2008

Keywords:
Pressure drop
Solid foam
Friction factor
Experimental data
Inertial parameter
Permeability

ABSTRACT

The use of porous structures with high external surface area represents an important breakthrough in industrial applications. Foam structures receive more and more scientific and industrial interest as catalyst support. Knowledge of pressure drop induced by these foam matrices is essential for successful design and operation of high performance industrial systems. In this context, the aim of this paper is to critically review the relation between permeability and structural parameters of the different foam structures. This work is willing to examine the effect of a large number of structural parameters (struts diameter, porosity, size of pores, specific surface area . . .) in the prediction of bed permeability based on principals of experimental and theoretical works on the single-phase flow model found in the literature. The state-of-the-art of modeling pressure drop in foams is summarized in Table 1. The goal was to assess and to critically evaluate all available design tools, whether empirical or theoretical.

1. Introduction

The use of porous structures with high external surface area represents an important breakthrough in industrial applications, especially in catalytic systems. The main advantage of using these porous structures is the high contact surface (specific surface) between the fluid and solid phase and also the low pressure drop along the catalyst bed. One eminent example is a packed bed, which is frequently utilized in catalytic converters and thermal energy storage device [1]. However, due to the low porosity (in the range of 0.3–0.6), packed bed induces an important pressure drop at high flow which is detrimental for the operating system, especially when high space velocity is required for maintaining acceptable selectivity. In addition, the conduction through the packed bed is less perfect as the particles in a packed bed were not well connected from each other but by local contact points; therefore, the effective thermal conductivity of such system is generally low and some heterogeneous temperature zones could be formed inside the catalyst bed [2]. It is then of interest to find new support materials which could remediate these drawbacks.

The idea of moving from the traditional packed bed, e.g. spheres, pellets, to the structured bed, i.e. monolith, wire or foam either made of stainless steel or ceramic, is becoming more and more popular during the last decade. Foam matrices have been recently introduced to overcome some of the above shortcomings dealing with the use of the packed bed. On the one hand, this new medium has a highly permeable porous structure with high porosity (0.60–0.95), which enables a considerable reduction of the pressure drop along the catalyst bed even at high gaseous space velocity and on the other hand, the solid ligaments (or struts) in foam material allows the continuous connection of the different catalyst domains which increase the effective thermal conductivity on the entire system without thermal breaking points as encountered with the packed bed.

The foam can be manufactured with different geometries and shapes, allowing for example the adjustment of axial or radial flow patterns in the reactor. The pore structure of a typical commercial product of foam, shown in Fig. 1, evidences a high degree of interconnectivity through the entire matrix of the foam. The small thickness of the struts or wall constituting the foam or monolith can allow the significant reduction of the diffusional phenomena reducing secondary reactions and by-products. Most characteristic parameters are the size of the windows (or pore diameter (a)), which is measured by several techniques and correlates with the pore density (the number of pores per linear inch, ppi) and the struts diameter (d_s).

Today, ceramic-based (Al_2O_3, cordierite, SiC . . .) and metals-based (aluminum, copper, etc.) cellular foams are widely used in a large range of applications, especially in the field of thermal applications (Lu et al. [3]). These peculiar structures are commonly applied for packaging of food, disposable hot-drinks cup (Gibson et al. [4]), packed cryogenic microsphere insulations, solar energy utilization, transpiration cooling, cavity wall insulation (Beavers et al. [5]). Solid foam structures also receive more and more scientific

* Corresponding author. Tel.: +33 390 242 675.
E-mail address: David.Edouard@ecpm.u-strasbg.fr (D. Edouard).

1385-8947/$ – see front matter © 2008 Elsevier B.V. All rights reserved.
doi:10.1016/j.cej.2008.06.007

Nomenclature

a	pore diameter (μm)
a_c	external specific surface (m^{-1})
d_s	strut diameter (μm)
d_p	particle diameter or equivalent diameter (μm)
$E_{1,2}$	Ergun constants
k_1	permeability coefficient (m^2)
k_2	inertial coefficient (m^{-1})
L	length of foam (m)
Re	Reynolds number
u	fluid velocity ($m\,s^{-1}$)

Greek letters

χ	tortuosity
ε	porosity
ρ_g	apparent density ($g\,l^{-1}$)
ρ_s	strut bulk density ($g\,l^{-1}$)
ΔP	pressure drop (Pa)

Subscripts

g	gas
l	liquid

and industrial interest as catalyst support for high space velocity reactions during the last decade. However, foam structures have a relatively low surface interaction and specific surface area for performing good anchorage and dispersion of the active phase and usually, a wash-coat layer of alumina is required for fulfilling such tasks. Recently, β-SiC foam with a medium specific surface area and a natural wash-coat layer, i.e. SiO_2 and SiO_xC_y topmost passivation layer (2–4 nm) formed by air oxidation of the ceramic at room temperature, has been synthesized and widely employed in several catalytic reactions (Ledoux et al. [6]). The passivation layer allows the good anchorage of the deposited active phase which enhance the number of active sites per linear surface while its low thickness allows the conservation of the intrinsic thermal conductivity of the underlying support (Winé et al. [7]). The main reason why reticulated foams are so attractive in the catalysis field is its high effectiveness in the heat and mass transfer properties along with the low-pressure drop (Richardson et al. [8], Groppi et al. [9]). The three-dimensional cellular structure of foam materials provided a turbulent mode of fluid flow, which significantly increased the extent of active surface utilization and catalyst efficiency. Permeability is also an important parameter for the characterization of foams employed in industrial applications. Knowledge of pressure drop induced by these foam matrices is essential for successful design and operation of high performance industrial systems. During the last decade, numerous experimental and theoretical models on single-phase flow in foams have been led. However, a strong discrepancy within the literature results appears today, which severely limits the development and validation of model of flow properties as a function of geometrical parameters of the used foam. Most of these studies, dealing with foam transport properties, were based on periodic structures which represent a low accuracy with respect to the real structure of the foam. The morphology of such open-celled matrices was characterized using struts diameter and/or pore size presented in Fig. 2 and the relative foam density.

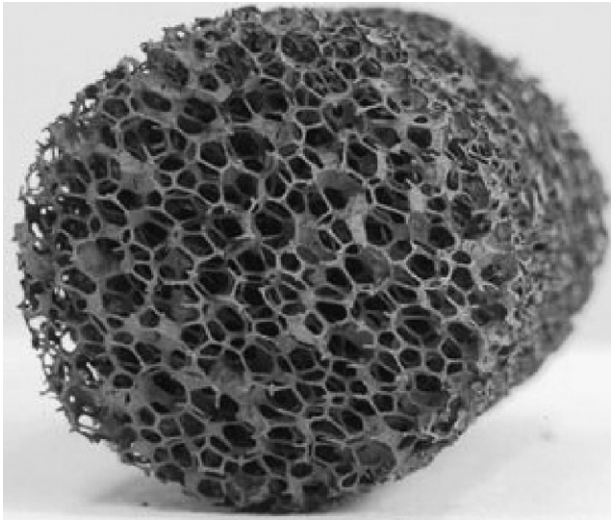

Fig. 1. SiC foam prepared by shape memory synthesis showing the well interconnection within the overall matrix.

In this context, the aim of this paper is to critically review the relation between permeability and structural parameters of the different foam structures. This work is willing to examine the effect of a large number of structural parameters (struts diameter, porosity, size of pores, specific surface area ...) in the prediction of bed permeability based on principals of experimental and theoretical works on the single-phase flow model found in the literature. The state-of-the-art of modeling pressure drop in foams is summarized in Table 1. The goal was to assess and to critically evaluate all available design tools, whether empirical or theoretical.

2. Characteristics of the foams and structural relationship

2.1. Morphological parameters

Several researchers have conduced experimental studies to correlate permeability with structural parameters of foam. However, due to the complexity of the geometric shape of these porous medium, there is no general consensus to define the main structural characteristics. Thus, the major problem in the permeability evaluation of foam is to define structural properties playing a role in pressure drop modeling. Today, in the literature survey [3,8–12], the permeability of the foams to gas flow can be related to macroscopic properties such as the number of pores per unit length, the apparent density, or the void fraction. The foams described in the literature, consist of a network of struts of materials (ceramic, metals, SiC, carbon ...). In Fig. 2, we can see that these struts are connected in vertices and surround the cells. These cells can be modeled for example by a dodecahedron [11,14], a polyhedra [13], tetrakaidecahedron [8,15], etc. This peculiar geometry is a consequence of the forming process of foams (replica technique [8,11,13,16,17]).

Macroscopic properties of these structures were accessible in routine measurements and as indicated in Fig. 2, generally three morphological parameters, namely respectively d_s (struts diameter), a (pores diameter) and ε (foam porosity) are used to describe the foams matrices.

The main morphological characteristics of foams were examined with an optical microscope and the diameters of the windows (or pores diameter, a) and the thickness of the struts (d_s) was measured by means of the sizing technique (see, for instance [8,11,13]).

The third important parameter of these structures is the foam porosity (ε) which is the volume available for the fluids flow through the open-cell structure. Generally in the literature, ε can be calculated on the basis of mass and volume measurements using the expression $\varepsilon = 1 - \rho_g/\rho_s$, where ρ_g is the foam apparent density and ρ_s is the materials density of the struts, which can be porous

Table 1
Original models and correlations

Reference	Relation between structural parameters	Specific surface area (m^2/m^3)	Pressure drop on foams correlation proposed
Giani et al. [10]	$d_s = a\left[\frac{4}{3\pi}(1-\varepsilon)\right]^{1/2}$	$a_c = \frac{4}{d_s}(1-\varepsilon)$	$\begin{cases} f = 0.87 + \frac{13.56}{Re} \quad \text{with} \quad Re = \frac{\rho d_s u}{\mu} \\ \frac{\Delta P}{L} = 13.56\frac{a^3}{2(a-d_s)^4 d_s}\mu u + 0.87\frac{a^3}{2(a-d_s)^4}\rho u^2 \end{cases}$
Lu et al. [3]	$d_s = a\left(\frac{2}{\sqrt{3\pi}}\right)[1-\varepsilon]^{1/2}$	$a_c = \left(\frac{2\sqrt{3\pi}}{a}\right)(1-\varepsilon)^{1/2}$	$f = \left[0.044 + \frac{0.008(a/d_s)}{(a/d_s-1)^{0.43+1.13(d_s/a)}}\right] Re^{-0.15}; Re = \frac{\rho d_s(u/1-d/a)}{\mu}$
Buciuman et al. [13]	$d_s = a\left[\frac{(1-\varepsilon)}{2.59}\right]^{1/2}$	$a_c = 4.82\frac{[1-\varepsilon]^{1/2}}{(a+d_s)}$	
Liu et al. [19]			$\begin{cases} f = 22\frac{(1-\varepsilon)}{Re} + 0.22 \quad \text{with} \quad d_p = 1.5a\frac{(1-\varepsilon)}{\varepsilon}; Re = \frac{\rho d_p u}{\mu} \\ \frac{\Delta P}{L} = 22\frac{(1-\varepsilon)^2}{\varepsilon^3 d_p^2}\mu u + 0.22\frac{(1-\varepsilon)}{\varepsilon^3 d_p}\rho u^2 \end{cases}$
Innocentini et al. [17]		$a_c = \frac{4(1-\varepsilon)}{\varepsilon a}$	$\begin{cases} f = 150\frac{(1-\varepsilon)}{Re} + 1.75 \quad \text{with} \quad d_p = 1.5a\frac{(1-\varepsilon)}{\varepsilon}; Re = \frac{\rho d_p u}{\mu} \\ \frac{\Delta P}{L} = 150\frac{(1-\varepsilon)^2}{\varepsilon^3 d_p^2}\mu u + 1.75\frac{(1-\varepsilon)}{\varepsilon^3 d_p}\rho u^2 \end{cases}$
Khayargoli et al. [26]			$\frac{\Delta P}{L} = 100\frac{(1-\varepsilon)^2}{\varepsilon^3 d_p^2}\mu u + 1\frac{(1-\varepsilon)}{\varepsilon^3 d_p}\rho u^2 \quad \text{with} \quad d_p = 1.5\frac{(1-\varepsilon)}{\varepsilon}a$
Richardson et al. [8]	$d_s = \frac{0.5338a(1-\varepsilon)^{0.5}}{1-0.971(1-\varepsilon)^{0.5}}$	$a_c = \frac{4\varepsilon}{a}$	$\begin{cases} \frac{\Delta P}{L} = \alpha\frac{s_v^2(1-\varepsilon)^2}{\varepsilon^3}\mu u + \beta\frac{s_v(1-\varepsilon)}{\varepsilon^3}\rho u^2; \alpha = 973a^{0.743}(1-\varepsilon)^{-0.0982}; s_v = \frac{12.98(1-0.971(1-\varepsilon)^{1/2})}{a(1-\varepsilon)^{1/2}}; \beta = 368a^{-0.7523}(1-\varepsilon)^{0.07158} \end{cases}$
Lacroix et al. [11]	$d_s = \frac{a[4/3\pi(1-\varepsilon)]^{1/2}}{1-[4/3\pi(1-\varepsilon)]^{1/2}}$	$a_c = \frac{4}{d_s}(1-\varepsilon)$	$\begin{cases} f = 150\frac{(1-\varepsilon)}{Re} + 1.75 \quad \text{with} \quad d_p = 1.5\,d_s; Re = \frac{\rho d_p u}{\mu} \\ \frac{\Delta P}{L} = 150\frac{(1-\varepsilon)^2}{\varepsilon^3 d_p^2}\mu u + 1.75\frac{(1-\varepsilon)}{\varepsilon^3 d_p}\rho u^2 \end{cases}$
Moreira et al. [16]			$\frac{\Delta P}{L} = 1.275\times10^9\frac{(1-\varepsilon)^2}{\varepsilon^3 a-0.05}\mu u + 1.89\times10^4\frac{(1-\varepsilon)}{\varepsilon^3 a-0.25}\rho u^2$
Fourie et al. [15], Du Plessis et al. [12]	$d_s = a\left(\frac{2}{3-\chi}-1\right)$	$a_c = \left(\frac{3}{a+d_s}\right)(3-\chi)(\chi-1)$ with $\chi = 2+2\cos\left(\frac{4\pi}{3}+\frac{1}{3}\cos^{-1}(2\varepsilon-1)\right)$	$\begin{cases} f = (3-\chi)(\chi-1)\frac{\rho_f\chi^2}{\mu\varepsilon^2(a+d_s)}\left[\frac{3A}{2}+\frac{B}{4}\right]u \\ A = \frac{24\varepsilon\mu}{\rho_f\chi(3-\chi)(a+d_s)u}; B = 1+10\left(\frac{\rho_f u(a+d_s)(\chi-1)}{2\mu\varepsilon}\right)^{-0.667} \\ \frac{\Delta P}{L} = \frac{36\chi(\chi-1)(3-\chi)^2}{\varepsilon^2 4a^2}\mu u + \frac{2.05\chi(\chi-1)}{\varepsilon^2 2a}\rho u^2 \end{cases}$
Tadrist et al. [20]			$\frac{\Delta P}{L} = c_1\frac{(1-\varepsilon)^2}{\varepsilon^3 d_s^2}\mu u + c_2\frac{(1-\varepsilon)}{\varepsilon^3 d_s}\rho u^2 \quad \text{with} \quad \begin{matrix} 100 \le c_1 \le 865 \\ 0.65 \le c_2 \le 2.6 \end{matrix}$
Topin et al. [25]			$\frac{\Delta P}{L} = \frac{1}{1.391\times10^{-4}}\frac{(1-\varepsilon)^2}{\varepsilon^3 d_s^2}\mu u + 1.32a_c\rho u^2$

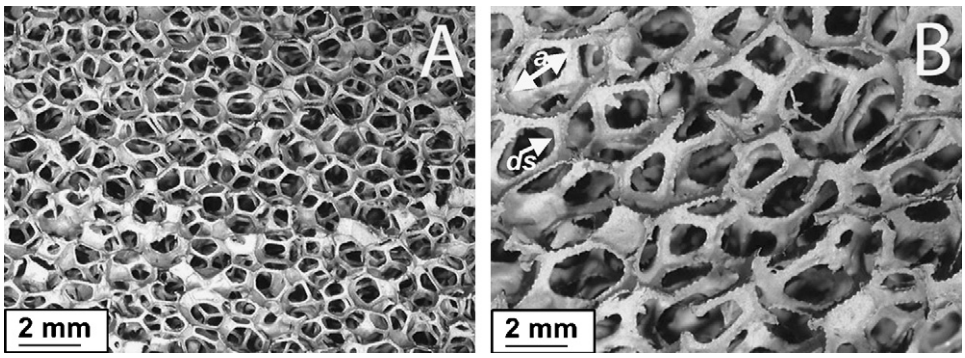

Fig. 2. Optical pictures of 740–780 μm (A) and 1600–1700 μm and (B) SiC foams showing the detail morphology and connection structure of the material.

with different pore size along the wall thickness [11] (Fig. 3). The material strut bulk density ρ_s and internal porosity can be obtained by different porous distribution techniques (mercury intrusion [11], water picnometer [13], He multipycnometer [8]). The ratio of mass to apparent volume of foams gives ρ_g.

Several researchers (see, for instance Table 1) reported theoretical geometrical models, which describe the relation between d_s, a and ε. Among all these approaches, a cubic cell model proposed by Lu et al. [3] in which the foam struts are represented as slender cylinders, representing the edges of an uniformly distributed cubic structure seem to reflect the real configuration of the foam in the best way. In the case of anisotropic foams, this model can be easily modified to consider a prism instead of a cube. Other models in the literature described the unit cell as dodecahedron structure [14], a tetrakaidecahedron [8,15] or a packing of polyhedra [13]. However, these models are more specific to special cases and due to the complex geometrical approaches, no general flow friction correlation for foam materials can be developed. Recently, Lacroix et al. [11] have shown that a modified cubic cell model developed by Giani et al. [10] combines simplicity and a good result for pressure drop estimation in the foam structure.

Although expressions for the strut diameters given in Table 1 exhibit the same dependence on the pore diameter, these relations show a difference of the dependence on the foam porosity. Note that in any case only two of the three parameters used for these different geometrical descriptions are independent. Fig. 4 compares the results of the dimensionless ratio d_s/a, which is calculated according to the equation presented in Table 1. We can see that for high porosity ($\varepsilon > 0.9$), different geometrical models give equivalent results, but in the porosity ranging between 0.6 and 0.9, the ratio d_s/a deviates quite significantly into two families by using the different theoretical geometrical models. Effectively, for one size of the given pores, Du Plessis et al. [15], Lacroix et al. [11] and Richardson et al. [8] find that the struts diameter (d_s) increase almost linearly and rapidly with decreasing foam porosity; while the increase of d_s seems less marked with the geometrical approaches used by Lu et al. [3], Giani et al. [10] and Buciuman et al. [13]. In the following sections, we will see that these differences in structural relationship can be responsible of errors in the estimated pressure drop modeling.

2.2. Theoretical and experimental specific surface area

For many industrial systems, external specific surface area (a_c, m^{-1} (i.e. m^2/m^3)) is an important parameter which is responsible for the high performance and successful design of reactors. For foam matrices, specific surface is typical higher than 2000 m^{-1} even at very low densities. For example, compact heat exchangers generally require $a_c > 700\,m^{-1}$ [18]. Thus, the foams are well qualified as "compact heat exchanger". Thus, foams are excellent candidates for many applications where size and weight of heat exchangers or reactors are limited due to design considerations

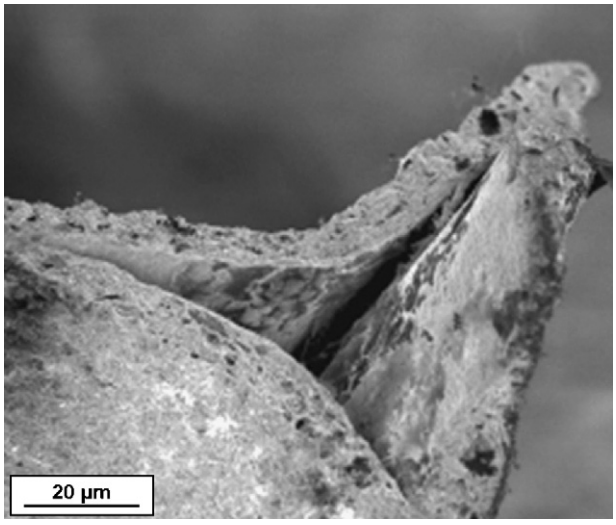

Fig. 3. SEM micrograph of the empty volume of a strut. This volume (obtained by the porous distribution delivered by mercury intrusion) must be withdrawn from the squeletal density.

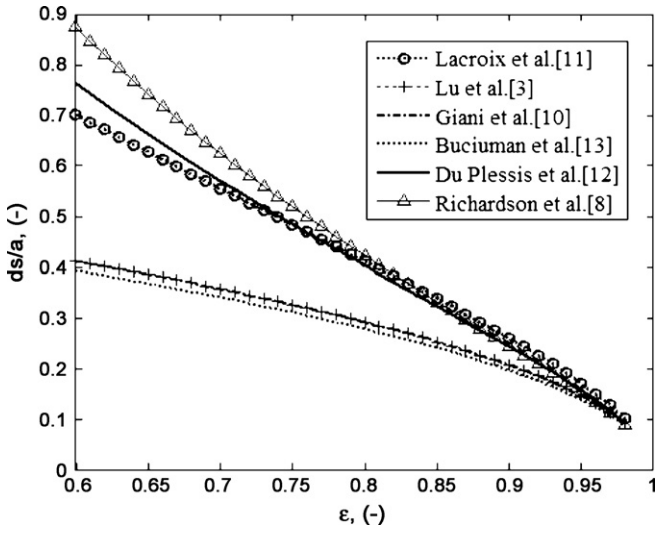

Fig. 4. Dimensionless ratio of strut diameter by pore diameter issue of the literature (Table 1).

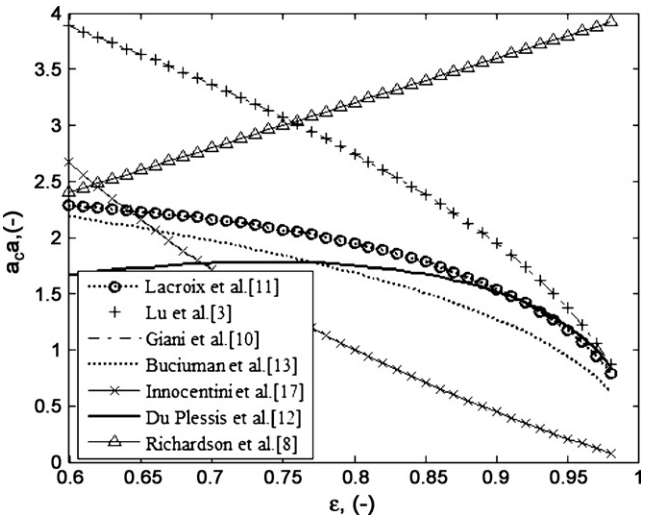

Fig. 5. Dimensionless specific surface versus foam porosity (Table 1).

(e.g. automotive, airborne equipments and air conditioners). For simple comparison, automotive radiators have $a_c \cong 600–1000\,m^{-1}$, cryogenic heat exchangers $1000–2000\,m^{-1}$, gas turbine rotary regenerators $3000–6000\,m^{-1}$, and human lungs $10^4\,m^{-1}$ [18]. Since a description of foam characteristics and pressure drop is greatly affected by the geometry interface, it is important that the value of the specific surface area (a_c, m^{-1}) is well calculated. In this section we examine different models proposed in the literature to calculate a_c (Table 1). The foams' specific surface area can be determined as a function of porosity and pore diameter and/or strut diameter. The main difference reported in Table 1 to calculate a_c is due to the different geometrical models used for describing the foam matrix. All expressions given in Table 1 presents a linearly dependence with the pore diameter. In Fig. 5, we have plotted the dimensionless product $a_c a$ versus the foam porosity (ε). Independently of the pore size, the evolution of the specific surface area as a function of the foam porosity follows two different behaviors. Effectively, when the porosity of the foam increases, in one case (Richardson et al. [8]) a_c also increases in a linear form while for the other studies, presented in Table 1, a_c decreases by a factor ranging between 2 and 4 according to the correlation used. The correlation developed by Richardson et al. [8] was also used by Liu et al. [19] and it was used only for ceramic foams with the typical porosity around 0.75 and thus seems valuable only for their own experimental studies. For other correlations, it can be noted that different models give results very close to each other except for the correlation made by Innocentini [17] which does not respond exponentially according to ε decreases. Only few authors compare the estimated specific surface area with the experimental data. Tadrist et al. [20] and Moreira et al. [16] measured the specific surface area by image analysis. The authors take into account the perimeters of the solid phase of a cross section of the foam and multiply it by the length. However, since each indicated value of specific surface area represents an average of image processing analyses, these results have a large incertitude range. Moreover in these works, the authors did not perform regression analysis to establish a correlation between specific surface area and characteristics of the used foams (i.e. d_s, a, ε). Hence, this measurement method seems weak in the case of foam matrices. Buciuman et al. [13] used the BET specific surface area (m^2/g) multiplied by the apparent densities (ρ_g) of the foams for comparing the theoretical specific surface area (m^{-1}). Authors obtained a good agreement between their correlation and experimental data in the case of a China porcelain foam, but a large deviation was observed taken the same correlation in the case of alumina-mullite foam. In the last case, the foam skeleton was formed upon diffusive sintering of the particles, thus the resulting struts became rougher. As the hollow struts are accessible for gas adsorption in BET measurement and that the geometrical model used to calculate the specific surface takes into account only the spatial arrangement and dimensions of the struts rather than their specific surface area characteristics, the difference between the experimental and calculated specific surface area give a direct information of the effects of surface roughness of foams (see for detail [13]).

Figs. 4 and 5 show that the selection of geometrical models for foam studies is not trivial. Before moving to the estimated pressure drop resulting from these correlations, we can note that the structural relationship (d_s/a and $a_c a$ versus ε) developed by Lacroix et al. [11], Fourie et al. [12], Du Plessis et al. [15] and Buciuman et al. [13] give a very close result with different approaches.

3. Single phase flow: pressure drop measurements and modeling on foams

The concept of permeability concept was first put forward by Henry Darcy in 1856 based on the laboratory tests performed with

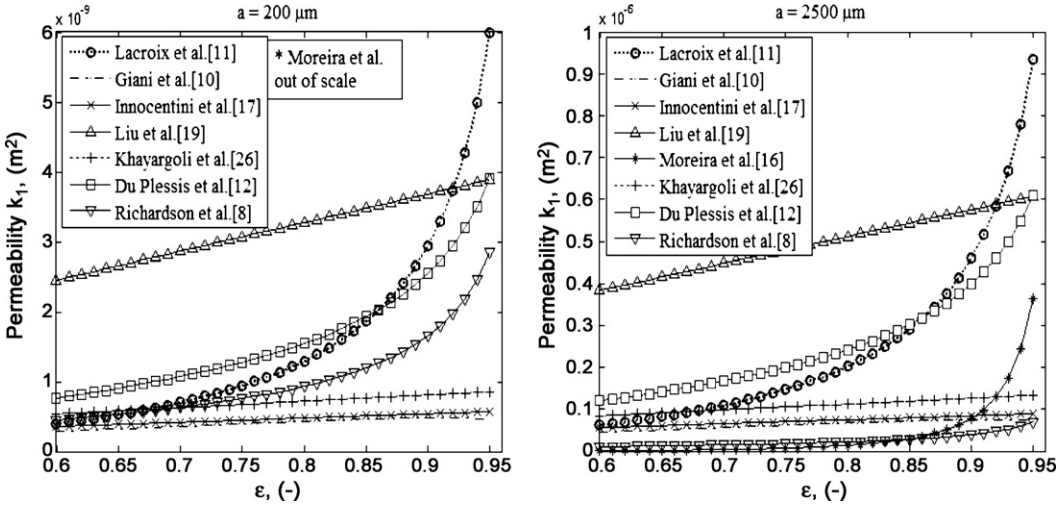

Fig. 6. Variation of permeability versus foam porosity for different pore diameters and correlations.

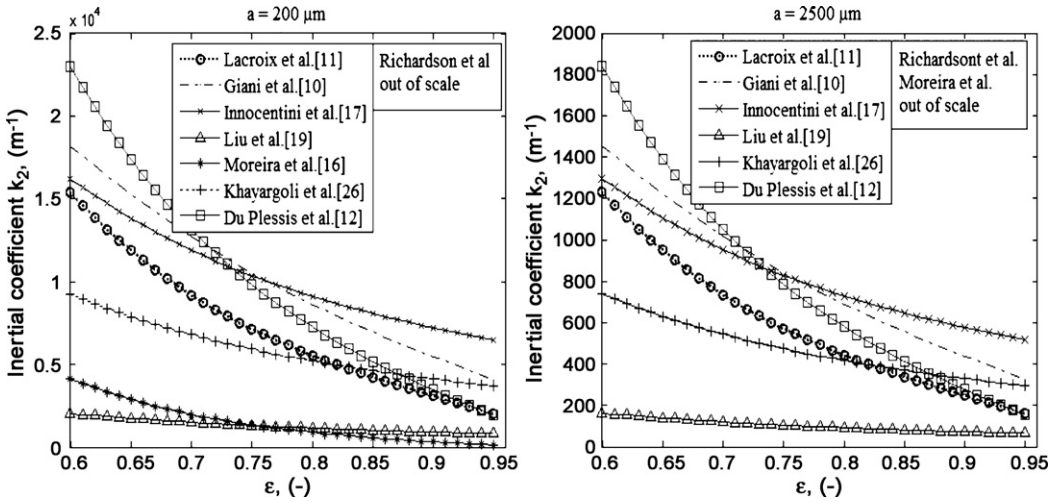

Fig. 7. Variation of inertial coefficient versus foam porosity for different pore diameters and correlations.

volumetric flow rate and pressure difference across a sand bed. Darcy proposed an empirical equation for estimating the volumetric flow rate (Q), given by:

$$Q = kA\frac{\mathrm{d}p}{\mathrm{d}x} \tag{1}$$

where k is the hydraulic conductivity, dx is the length of the porous medium, dp is the hydrostatic pressure drop and A is the cross section area. However, this first equation was limited to incompressible and isothermal flow of Newtonian fluids. Hazen [21] first proposed modifications to Darcy's law in order to include temperature although viscous effects. Since then, several researches have verified and completed the Darcy's law and the permeability of a fluid while flowing through a porous medium is usually quantified by the Forchheimer equation, described as:

$$\frac{\Delta P}{L} = \frac{1}{k_1}\mu u + k_2\rho u^2 \tag{2}$$

where ΔP is the pressure drop, L is thickness of the medium, ρ and μ are the density and the viscosity, respectively and u the velocity of the flowing fluid. k_1 and k_2 are usually referred to as the Darcyan and non-Darcyan permeability parameters, respectively. These parameters are assumed to be only a function of bed characteristics and in case of foam matrices, represent the structural properties developed in previous section. Generally, pressure drop measurement presented in the literature confirmed that foam matrices follow the Forscheimer relationship. Due to the difficulties in identifying structural characteristics that represent these porous media, most of the models used to determine permeability in foam matrices are derived from correlations originally developed for granular beds, and thus, could induced a large deviation with the experimental data.

The pressure drop is the sum of viscous and inertial terms and several researches adopted Erguns' like models to explain and fit their experimental data ([8,16,17] for example). Ergun, proposed in 1952 the following correlation to estimate the pressure drop for packed bed made of spheres [22]:

$$\frac{\Delta P}{L} = E_1\frac{\mu(1-\varepsilon)^2 u}{\varepsilon^3 d_\mathrm{p}^2} + E_2\frac{\rho(1-\varepsilon)u^2}{\varepsilon^3 d_\mathrm{p}} \tag{3}$$

where u is the fluid velocity (m s^{-1}), ΔP the pressure drop (Pa), L the length of the porous medium (m), μ and ρ are the fluid viscosity and fluid density respectively, E_1 and E_2 are Ergun constants,

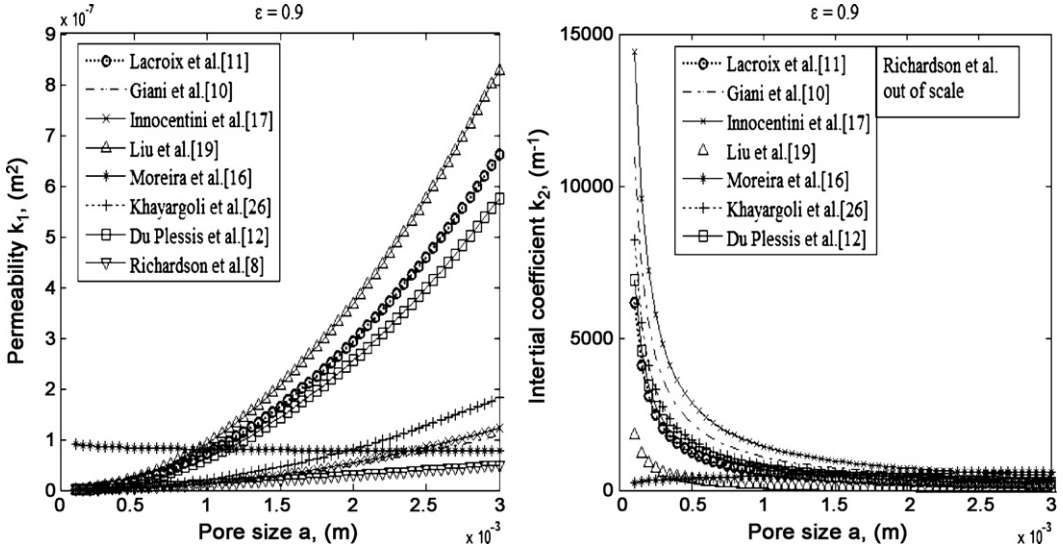

Fig. 8. Variation of k_1 and k_2 versus pore diameter with two foam porosities.

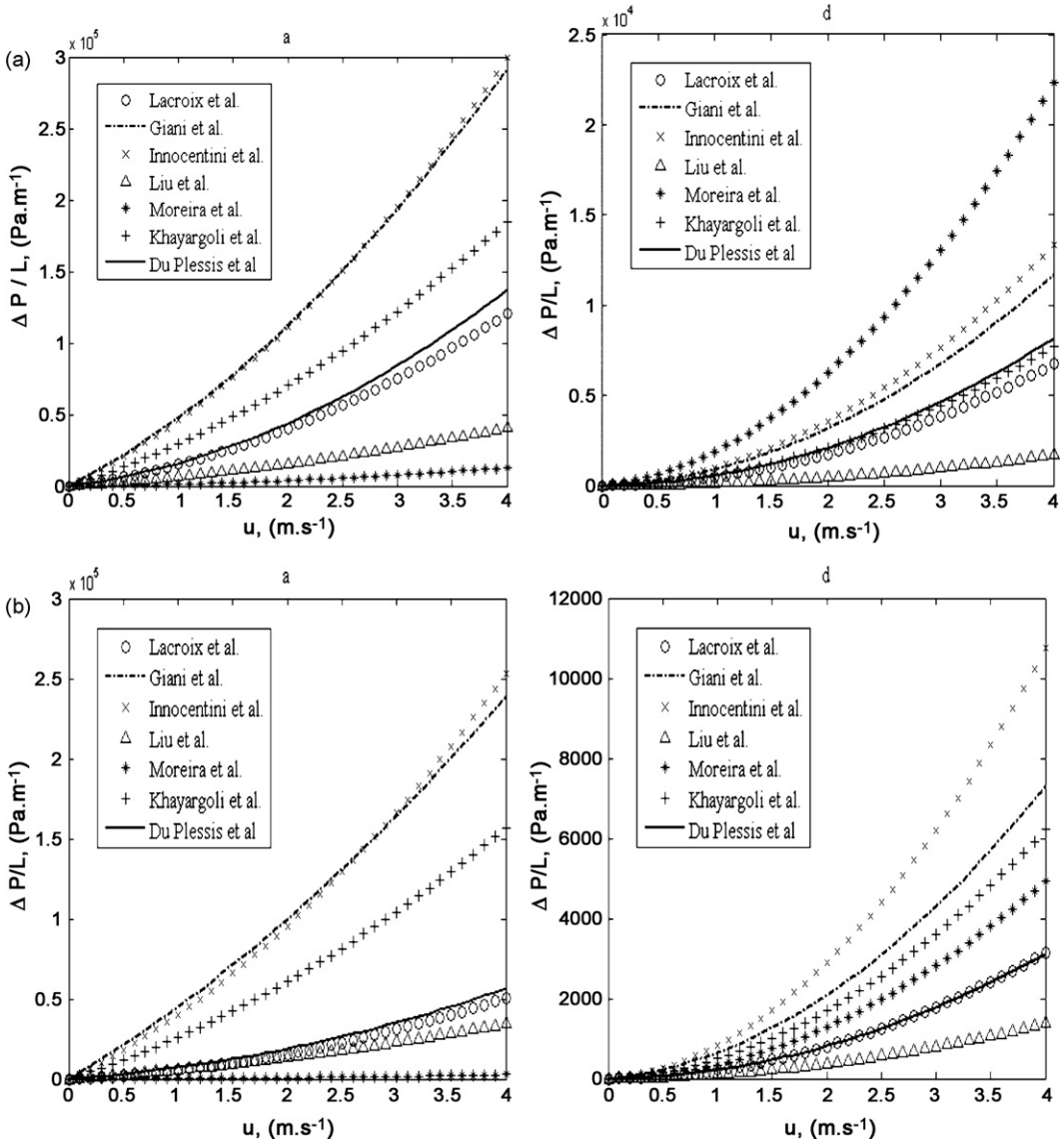

Fig. 9. (a) Estimated pressure drop versus gas superficial velocity for $\varepsilon = 0.85$ and two pore diameter given: $a = 200\ \mu m$ and $d = 2500\ \mu m$. (b) Estimated pressure drop versus gas superficial velocity for $\varepsilon = 0.95$ and two pore diameter given: $a = 200\ \mu m$ and $d = 2500\ \mu m$.

ε is the bed porosity and d_p is the mean particle diameter of the granular medium. The first term in this Eq. (3) can be used to estimate permeability as $k_1 = \varepsilon^3 d_p^2/E_1(1-\varepsilon)^2$ and comparison of the inertial term in Eqs. (2) and (3) give the direct following relation for the drag force coefficient of the porous media: $k_2 = E_2(1-\varepsilon)/\varepsilon^3 d_p$. In the literature, the constants E_1 and E_2 in the above equations are not considered as "universal", but depend on the nature of the porous media. In many practical cases, the Ergun constants depend on the packing properties (spheres, extrudates, slabs, etc. (see, for instance Iliuta et al. [23])). These constants can be determined by measuring single-phase gas flow pressure drops (Holub et al. [24]) or estimated from literature correlations. However, from many experimental data, Ergun proposed the following value for packed columns made of spheres: $E_1 = 150$ and $E_2 = 1.75$.

The major problem in the foam pressure drop estimation is to reliably define structural properties of porous medium in order to replace the equivalent particle diameter (d_p) in Eq. (3). Several approaches have been proposed in the literature to tackle this problem. From Eq. (2) (or similar form), most authors optimize parameters k_1 and k_2 in order to fit their experimental data with those of the theories. The optimal values obtained were further discussed as a function of the porosity and the pore sizes for different foams. Table 1 summarizes the principal correlations available in the literature. Values of E_1 and E_2 resulting from these approaches and used in these correlations comprised between 100 to 865 and 0.65 to 2.65, respectively. At first sight, these large ranges suggest that the Ergun-like model is not suitable. However, Fourie et al. [15], Du Plessis et al. [12] and more recently Lacroix et al. [11] have developed models to estimate the pressure drop without optimization. In the work of Lacroix et al. [11], a simple analogy between the traditional spherical particle bed and the foam was proposed in order to predict the pressure drops in foams through standard Ergun's equation.

3.1. Results and discussion of calculation of pressure drop on foams

Another form of Ergun's equation is also often used in the literature to describe the pressure drop characteristic of various types

Table 2
Characteristics of the solid foam samples and experimental values of the inertial parameter and permeability

Author	Sample reference	Material characteristics			ε	$k_{1,\mathrm{exp}}$	$k_{2,\mathrm{exp}}$	$k_{1,\mathrm{th}}$[a]	$k_{2,\mathrm{th}}$[a]
		a [m]	d_s [m]	PPI					
Giani et al. [10]	Sample B	4.70×10^{-3}	8.20×10^{-4}	5.4	0.927	–	161.58	–	200.78
	Sample C	2.20×10^{-3}	3.70×10^{-4}	11.5	0.938	–	531.93	–	401.36
	Sample D	2.00×10^{-3}	3.30×10^{-4}	12.8	0.937	–	621.92	–	444.25
	Sample F	4.60×10^{-3}	8.00×10^{-4}	5.6	0.911	–	285.22	–	224.47
Liu et al. [19]	Sample 1	1.21×10^{-3}		5	0.914	3.70×10^{-7}	164.07	1.36×10^{-7}	145.34
	Sample 2	1.19×10^{-3}		10	0.918	6.23×10^{-7}	230.58	1.33×10^{-7}	146.25
	Sample 3	8.27×10^{-4}		20	0.870	1.25×10^{-7}	280.86	6.09×10^{-8}	234.31
	Sample 4	8.05×10^{-4}		20	0.909	1.02×10^{-7}	231.08	6.02×10^{-8}	220.50
	Sample 5	8.14×10^{-4}		20	0.935	2.42×10^{-7}	264.26	6.34×10^{-8}	206.10
	Sample 6	8.00×10^{-4}		20	0.958	1.42×10^{-6}	285.32	6.27×10^{-8}	199.76
	Sample 7	6.85×10^{-4}		40	0.935	1.33×10^{-7}	282.43	4.49×10^{-8}	244.92
Innocentini et al. [17]	30 PPI	9.28×10^{-4}		30	0.890	3.20×10^{-8}	1587.30	3.20×10^{-8}	951.33
	45 PPI	1.28×10^{-3}		45	0.880	2.56×10^{-8}	1176.47	2.56×10^{-8}	1081.80
	60 PPI	2.91×10^{-4}		60	0.850	5.10×10^{-9}	5555.56	5.10×10^{-9}	2553.17
	75 PPI	1.61×10^{-4}		75	0.850	3.90×10^{-9}	10000.00	3.90×10^{-9}	2919.66
Lacroix et al. [11]	SiC 1750 μm, $e = 0.91$	1.78×10^{-3}			0.915	2.75×10^{-7}	311.04	2.75×10^{-7}	311.04
	SiC 2650 μm, $e = 0.91$	2.68×10^{-3}			0.910	5.89×10^{-7}	214.43	5.89×10^{-7}	214.42
	SiC 3650 μm, $e = 0.91$	3.68×10^{-3}			0.914	1.16×10^{-6}	151.40	1.16×10^{-6}	151.40
	SiC 1750 μm, $e = 0.89$	1.78×10^{-3}			0.890	2.09×10^{-7}	372.10	2.09×10^{-7}	372.09
	SiC 1750 μm, $e = 0.81$	1.78×10^{-3}			0.810	1.09×10^{-7}	592.53	1.09×10^{-7}	592.52
Du Plessis et al. [12]	G100	2.53×10^{-4}	$\chi = 1.1962$	100	0.973	1.77×10^{-9}	2252.96	8.81×10^{-9}	1004.72
	G60	5.22×10^{-4}	$\chi = 1.1885$	60	0.975	8.00×10^{-9}	1025.29	3.91×10^{-8}	463.21
	G45	7.14×10^{-4}	$\chi = 1.1765$	45	0.978	1.60×10^{-8}	696.46	7.84×10^{-8}	311.92
Topin et al. [25]	NC 3743	5.69×10^{-4}			0.870	2.13×10^{-9}	1330.00	1.75×10^{-9}	1386.58
	NC 2733	8.31×10^{-4}			0.910	4.44×10^{-9}	1075.00	8.94×10^{-9}	628.40
	NC 1723	1.84×10^{-3}			0.880	2.81×10^{-8}	490.00	2.23×10^{-8}	391.30
	NC 1116	2.45×10^{-3}			0.890	6.02×10^{-8}	381.00	4.87×10^{-8}	266.14
Khayargoli et al. [26]	NC 4753	4×10^{-4}			0.86	1.62×10^{-9}	2274.44	3.09×10^{-9}	2253.47
	NC 3743	5×10^{-4}			0.83	3.54×10^{-9}	1748.12	4.66×10^{-9}	1935.45
	NC 2733	6×10^{-4}			0.9	5.01×10^{-9}	1203.01	7.29×10^{-9}	1371.74
	NCX 1723	9×10^{-4}			0.885	1.53×10^{-8}	488.722	1.61×10^{-8}	945.76
	NCX 1116	1.4×10^{-3}			0.9	2.74×10^{-8}	357.143	3.96×10^{-8}	587.89
Richardson et al. [8]	99.5 wt.% Al_2O_3 without wash-coat 10 PPI	1.68×10^{-3}		10	0.878	1.93×10^{-8}	122.82	1.49×10^{-8}	119.57
	99.5 wt.% Al_2O_3 without wash-coat 30 PPI	8.26×10^{-4}		30	0.874	4.82×10^{-9}	431.03	6.10×10^{-9}	419.63
	99.5 wt.% Al_2O_3 without wash-coat 45 PPI	6.19×10^{-4}		45	0.802	3.96×10^{-9}	876.55	4.07×10^{-9}	853.37
	99.5 wt.% Al_2O_3 without wash-coat 65 PPI	3.59×10^{-4}		65	0.857	2.39×10^{-9}	1948.22	2.13×10^{-9}	1896.68

[a] With authors' model.

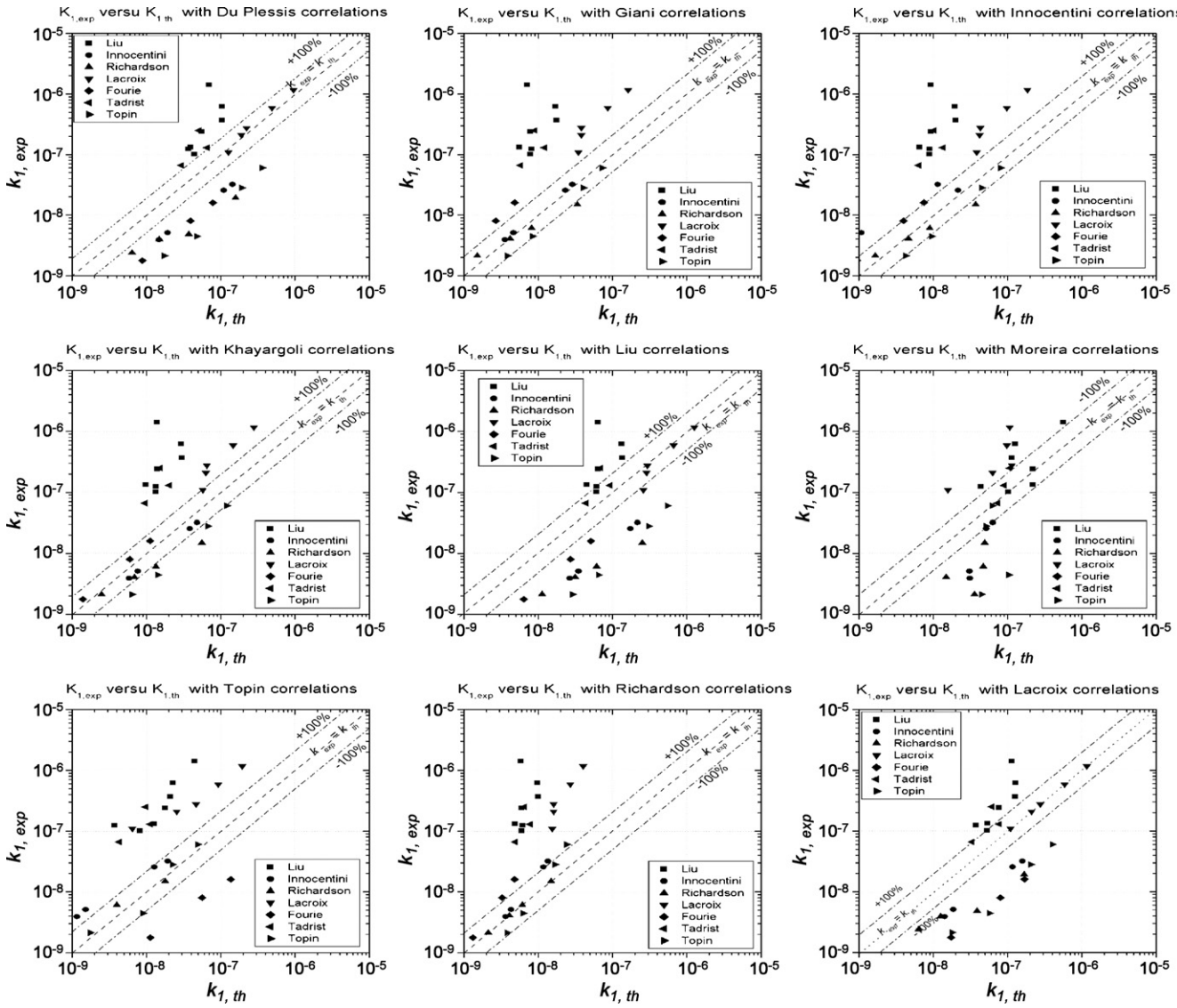

Fig. 10. Parity diagrams: experimental values of k_1 versus values calculated with different models.

of granular porous materials (Eq. (4)):

$$f = 150\frac{(1-\varepsilon)}{Re} + 1.75 \tag{4}$$

where f is the friction factor given by: $f=(\Delta P/L)(d_p\varepsilon^3/\rho u^2)(1-\varepsilon)$ and Re is the Reynolds number.

The Reynolds number is strongly dependent on d_p and reflected the geometrical approaches used by the authors. From Table 1, we observe that d_p is defined by different relationships according to the work issue of the literature. Therefore, for a given pore size, strut diameter and foam porosity, we can obtain different values of d_p and thus different values of the corresponding Reynolds number. This remark can be explained by the fact that in literature [19], a large divergence was observed by different authors when the friction factor was plotted versus the Reynolds number. Consequently, it is not suitable to use this typical form to discuss the results of the pressure drop in foam determined by different correlations cited in Table 1. Figs. 6 and 7 display variations of permeability (k_1) and inertial coefficient (k_2) versus the porosity of foam at different size of pores (a) given. These figures represent the results of calculations for eight correlations presented in Table 1 and for two pores diameter (a = 200 and 2500 μm). Fig. 8 shows k_1 and k_2 versus pore size for a given foam porosity (ε = 0.9). Finally, Fig. 9 displays variations of the pressure drop per unit length (L) of the foam versus the velocity (u) at a different given foam porosity and pore size (a). Although $\Delta P/L$ vary between 0.01 and 3 in these calculations and in this condition flow compressibility effects are non-negligible (Topin et al. [25]), the theory estimated pressure drop in this study did not take the fluid compressibility into account. Fig. 9 represents the results of pressure drop for seven correlations presented in Table 1 and for two different foam porosities (ε = 0.85 and 0.95) and two pore diameters (a = 200 and 2500 (m). The gas used for pressure drop calculation was air, and the inlet pressure was atmospheric pressure. In these calculations, air properties were assumed constant for the whole range of considered pressure and the values are given by: ρ_{gas} = 1.2 kg m^{-3} and $\mu_{gas} = 1.838 \times 10^{-5}$ Pa s.

All these different results presented (Figs. 6–9) were well agreed with the typical results of the literature:

- Permeability k_1 increases and k_2 decreases with the increase of foam porosity, in other terms the pressure drop on foam decreases when the foam porosity increases for a given pores diameter.

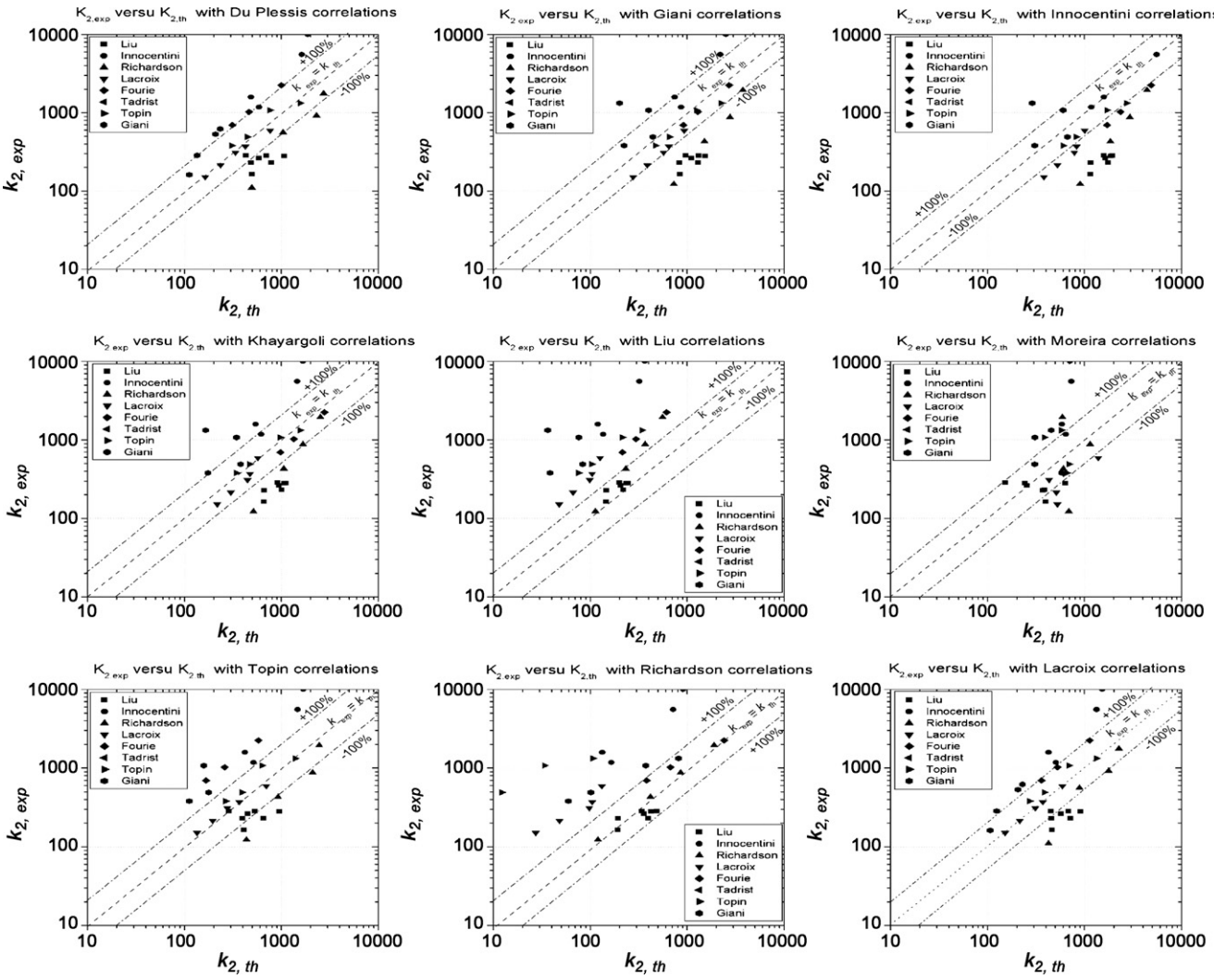

Fig. 11. Parity diagrams: experimental values of k_2 versus values calculated with different models.

- On the other hand, expected from the correlation of Moreira, k_1 increases and k_2 decreases as the pore size increases (i.e. pressure drop decreases for fixed porosity with pores diameter increases).

The variation of the permeability (k_1) as a function of the porosity and the pore size estimated by Richardson correlation agrees with other correlation. However, it is noteworthy that the values of k_2 obtained with this correlation were out of scale. The fitting parameter β involves in inertial terms need to be optimized by the authors for high velocity which can explain this difference with other results of calculation. The others results of calculation for the inertial term (k_2) with foam porosity obtained by correlations of Giani et al. [10], Innocentini et al. [17], Khayargoli et al. [26], Du Plessis et al. [12,15] and Lacroix et al. [11] were very close from each other. Fig. 7 shows that Du Plessis and Khayargoli correlations give the most and least variation respectively of k_2 according to ε. According to the results in Fig. 8, the variation of k_2 versus a was identical with a similar form for these correlations in a case where $a > 1000$ μm. Always for these correlations, the variation of permeability (k_1) with ε and a is different (Figs. 6 and 8). Effectively, Du Plessis and Lacroix correlations show an exponential form variation of permeability while for other works (Giani, Innocentini and Khayargoli correlations) the permeability seems to increase with a linear form.

From these results, Fig. 9(a and b) show that a small variation in the calculation of permeability (k_1 or k_2) can induce a large different on pressure drop. Effectively, we can see that the correlation of Moreira et al. [16] gives the weakest pressure drop in all the cases of small pores diameter and highest in the case of large pores diameter except in case of high porosity (i.e. $\varepsilon > 0.95$). Apparently, due to the fact that this correlation has been obtained by fitting only three experiments at low fluid velocity and that it was relatively sensitive to the size of the pore diameter, it seems not to be valid in a large range of solid foam and experimental conditions.

Correlation of Liu et al. [19] gives the lowest estimation of pressure drop in all calculations (Fig. 9). In their studies, the experimental data have obtained with aluminum foams with high porosity ($\varepsilon > 0.9$). The fitting correlation was developed from these measurements at high Reynolds number and was validated with a variation of more than 30% compared to the data of Du plessis et al. [12,15] and Richardson et al. [8]. Only in the case where the foam porosity was higher than 0.9, the estimated pressure drop with this correlation can be compared with the different one. This large discrepancy in estimation of coefficient k_1 and k_2 can be explained by the determination of the equivalent spherical diameter used in the Ergun's equation. Due to the fact that the nominal numerical Ergun constants (E_1 and E_2) were replaced by another optimal (fit-

ting) numerical values (respectively 22 and 0.22 instead of 150 and 1.75), we expected that this model did not give a general equation for the estimation of the pressure drop through different foam matrices.

Correlation of Giani has been obtained by fitting based on the measurement of pressure drop on four metal foam samples with high porosity ($\varepsilon > 0.92$) and low pore size ($a < 500\,\mu m$). This correlation was based on Ergun's equation with numerical Ergun constants which is different from the original values. In this work, the strut diameter (d_s) was validated as the appropriate characteristics for simulating the pressure drop in foam matrices. Innocentini based their modelization first on a direct Ergun's equation but used another equation for obtaining an equivalent spherical particle size from the measurement of mean pore diameter. Authors compared their estimation of pressure drop with four SiC–Al_2O_3 foam samples ($0.85 < \varepsilon < 0.89$) and noted that the use of Ergun's equation as originally proposed yield errors in the prediction of permeability of foam matrices as high as 50%. The direct introductions of pore size obtained by image analysis for each foam sample seem to be necessary. Khayargoli used a direct Ergun's equation with the same relationship between pore diameter and equivalent spherical particle described by Innocentini. In this work too, the best data fit has been obtained with Ergun constants which are different from the proposed original values.

For two given porosity values ((= 0.85 and 0.95) and especially for a high value of pore size ($a = 2500\,\mu m$), we can see that the results of correlations proposed by Lacroix et al. [11] and Du Plessis et al. [12,15] were relatively close and deviated from the results of the other correlations. These two studies were not based on any optimization and rely only on the geometrical approaches which were, however, different. Du Plessis et al. [15] used the concept of a rectangular representative unit cell with a tetrakaidecahedron structure model to obtain expression of the geometric tortuosity (given by χ in Table 1). From this parameter, Du Plessis obtained the permeability and the inertial terms of Forchheimer equation. Their study was validated by experimental data for samples with a small pore size and high porosity, using water and glycerol as the fluid phase. Lacroix et al. [11] used a modified cubic cell model introduced by Giani [10] with Ergun's equation and used the standard Ergun parameters constant ($E_1 = 150$ and $E_2 = 1.75$). This work has evaluated the applicability of analogy between the traditional spherical particles bed and the foam in order to predict the pressure drops in foams through standard Ergun's equation. A direct analogy between foams and beds made of spherical particles with the same specific surface area and same porosity than foam was developed through a simple equation ($d_p = 3/2d_s$). The estimated pressure drop results were compared with those obtained experimentally under air flow on SiC foams with pores diameter (a) ranging between 475 and 1650 μm, porosity between 0.76 and 0.92 and from fluid velocities as high as $6\,m\,s^{-1}$.

The results of calculation of other correlations proposed in this review (Tadrist et al. [20] and Topin et al. [25]) were not presented. Effectively, on one hand, the fitted parameters involved in these correlations fluctuate in a relatively large range ($100 \le c_1 \le 865$ and $0.65 \le c_2 \le 2.6$) and, on the other hand, no relationship is given to estimate the specific surface area used in Topin pressure drop correlation. It is interesting to note that for any correlation proposed in open literature, the direct introduction of pore size or strut diameter obtained by image analysis for each foam sample can be used as primary input in order to reconcile theory and experimental data.

In the following section, we develop a comparison of experimental data reported in the open literature with results obtained by these correlations.

3.2. Comparisons of literature data with main presented correlations

The experimental data of k_1 and k_2 were collected from literature presented in Table 1 and compiled in Table 2 with the studied foams characteristics (pore size, porosity, strut size and tortuosity when available). The experimental values of k_1 and k_2 (obtained by fitting experimental data of pressure drop versus fluid velocity using Forschheimer equation) were compared with the theoretical values obtained using the authors' model. It appears in this table that the theoretical values obtained by the authors are generally close to the experimental ones. The experimental value of k_1 and k_2 were then compared with the values that would be obtained using the different cited models in order to check the validity of these models with other experimental data. Fig. 10 present the plot of experimental value of $k_{1,exp}$ versus value of $k_{1,th}$ calculated with the different available correlations. The same plot is done for k_2 on Fig. 11. From Fig. 10, it appears that no model is perfect: the best models give theoretical value of k_1 in the same range than the experimental ones but no perfect match is found for any model. Some models underestimate most theoretical values of k_1, like Richardson [8], Innocentini [17] and Giani [10] (points above the diagonal) and to a lower extent Khayargoli [26] and Topin [25]. Some other models overestimate theoretical value of k_1, in particular Liu et al. [19] model. Moreira's model [16] gives nearly the same theoretical value of k_1 (around 8×10^{-7}), whereas the range of experimental data is from 10^{-9} to 10^{-6}. Du Plessis et al. [12] and Lacroix et al. [11] models give theoretical values of k_1 close to each other and with the lower standard deviation between experimental and theoretical values.

In the same way, it appears on Fig. 11 that no model is perfect for the determination of the non-Darcian parameter k_2. Liu [19] and Richardson [8] models underestimate most values of k_2 (most points above diagonal). In the other way, Innocentini et al. model [17] overestimates k_2 value (points below diagonal). Moreira et al. model [16] gives theoretical value of k_2 close to 500 for any foams. This may be explained by the fact that the pore size has little effect in this model (a to the power −0.25). Finally, other models (Du Plessis et al. [12], Giani et al. [10], Khayargoli et al. [26] and Lacroix et al. [11]) give theoretical values of k_2 close to each other and with "low" standard deviation between experimental and theoretical data.

It is interesting to underline the fact that the authors for whom $k_{1,th}$ is overestimated present underestimated $k_{2,th}$ values and reciprocally. This was attributed to the fact that $k_{1,th}$ was proportional to a^2 and $k_{2,th}$ was proportional to a^{-1} in many correlations. The uncertainties on the experimental pore size can then explain the deviation from the presented correlations because they are very sensitive to the pore size. Moreover, it is well known that the measurement of the pore size is not an easy task and can present large uncertainties due to some geometrical anisotropy (Innocentini et al. [17], Du Plessis et al. [12], Bhattacharya et al. [14] and Lacroix et al. [11]); then, one can measure a mean value of the pore size but the smallest pores will impose the value of the pressure drop over the whole sample; moreover, the pore size was not always clearly defined in the different works. Effectively, some authors describe it as the size of the unit geometrical cell of the medium and some other as the size of window of this same cell. Finally, most authors have large uncertainties on the experimental value of $k_{1,exp}$ (see for example Innocentini et al. [17]) due to the fact that $k_{1,exp}$ and $k_{2,exp}$ were not directly measured but they were estimated from the measurement of pressure drop versus fluid velocity using the Forschheimer equation.

Finally, if reliable values of both k_1 and k_2 values are expected, we would recommend the use of Du Plessis [12] and Lacroix

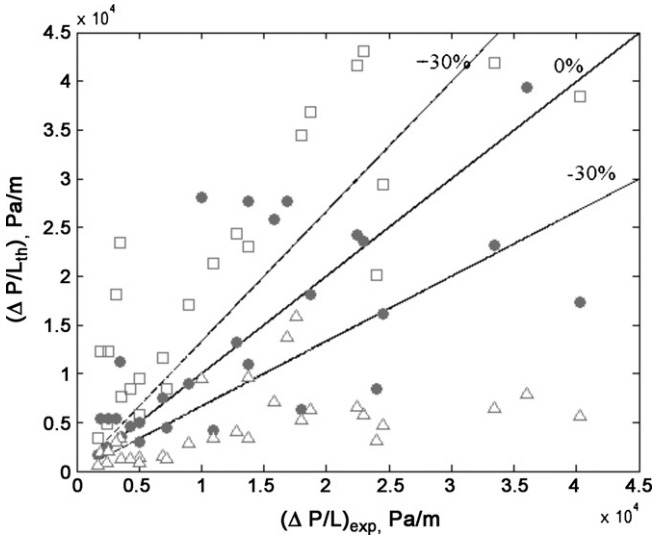

Fig. 12. Parity diagram of pressure drop. Theoretical value versus experimental data. (●) Lacroix et al. [11], (□) Giani et al. [10], (Δ) Liu et al. [19].

[11] models. These models are based on morphological parameters of the foams (porosity, strut size) and can be applied to any kind of foam (metallic, ceramic, carbon plastic, etc.) without the use of any fitting method. The two correlations give estimation of k_1 and k_2 close to each other although the two approaches remain different. Moreover these correlations give a relative "low" standard deviation between experimental and theoretical values.

As mentioned in the previous section, an error in calculation of k_1 and/or k_2 can induce a large difference between pressure drop measurements and calculated values. So, in practical view, it is interesting to compare the experimental data of pressure drop with the theoretical values obtained from $k_{1,th}$ and $k_{2,th}$. Fig. 12 presents the plot of calculated pressure drop with Lacroix, Giani and Liu correlations versus experimental pressure drop. Experimental data are directly calculated from $k_{1,exp}$ and $k_{2,exp}$ presented in Table 2 (except for Innocentini et al. [17]) and considering two velocities of gas (air): 3 and 7 m/s. From this figure and the previous results for $k_{1,th}$ and $k_{2,th}$, it is easy to see that Giani correlation overestimated the pressure drop while Liu correlation underestimated these values. Lacroix correlation gives a relatively low standard deviation between experimental and theoretical values with the majority of pressure drop data lying in the ±30% region.

Finally, all the expressions for the strut diameters given in Table 1 exhibit the same dependence on the pore diameter and show only a difference for the dependence on the foam porosity. Moreover as indicated in the previous section, in any case only two of three parameters (a, d_s and ε) used for these different descriptions of solid foam are independent. Thus at first glance, we can think that it is possible to use the pore diameter or the strut diameter as the characteristic size of the foam unit cell. However, the results of this review work demonstrate that the pore diameter was not the appropriate characteristics in order to model the pressure drop on foams but that the strut diameter can be more appropriate for calculating the pressure drop with standard Ergun's equation on foam matrices.

4. Conclusions

On one hand, based on the main experimental and theoretical works of the literature, state-of-art examines the effect of morphology of the foam (struts and pores diameter, exchange specific surface area . . .) in the prediction of bed permeability for different types of solid foams. It appears from this study that no model is perfect and that the standard deviation between experimental and theoretical values can be as high as 100%. Among all correlations presented in this review, the approaches proposed by Du Plessis and Lacroix seem to be more adapted to estimate the pressure drop within foam structure since they do not involve any fitting of the data. Although these correlations are based on approaches which use different physical characteristics (tortuosity or strut diameter), they present estimation of k_1 and k_2 close to each other and give a relative "low" standard deviation between experimental and theoretical values with the majority of pressure drop data lying in the ±30% region.

Acknowledgements

The authors would like to thank the SiCat Co. and Total SA for technical and financial support.

References

[1] F.W. Schmidt, A.J. Willmott, Thermal Energy Storage and Regeneration, McGraw-Hill, New York, 1981.
[2] K. Ofuchi, D. Kunii, Int. J. Heat Mass Transfer 8 (1965) 749.
[3] T.J. Lu, H.A. Stone, et al., Heat transfer in open-cell metal foams, Acta Mater. 46 (10) (1998) 3619–3635.
[4] L.J. Gibson, M.F. Ashby, Cellular Solids, Cambridge University Press, Cambridge, 1997.
[5] G.S. Beavers, E.M. Sparrow, J. Appl. Mech. 36 (1969) 711.
[6] M. Ledoux, J. Pham-Huu C, Silicon carbide: a novel catalyst support for heterogenous catalysis, CaTTech 5 (2001) 226–246.
[7] G. Winé, J.P. Tessonier, S. Rigolet, C.L. Marichal, M.J. Ledoux, C. Pham-Huu, Beta zeolite supported on a SiC foam: a diffusionless catalyst for fixed-bed Friedel-Crafts reactions, J. Mol. Catal. A: Chem. 248 (2006) 113–120.
[8] J.T. Richardson, Y. Peng, D. Remue, Properties of ceramic foam catalyst supports: pressure drop, Appl. Catal. A: Gen. 204 (2000) 19–32.
[9] G. Groppi, E. Tronconi, Design of novel monolith catalyst supports for gas/solid reactions with heat exchange, Chem. Eng. Sci. 55 (12) (2000) 2161–2171.
[10] L. Giani, G. Groppi, et al., Mass-transfer characterization of metallic foams as supports for structured catalysts, Ind. Eng. Chem. Res. 44 (2005) 4993–5002.
[11] M. Lacroix, P. Nguyen, D. Schweich, C. Pham Huu, S. Savin-Poncet, D. Edouard, Pressure drop measurements and modelling on SiC foams, Chem. Eng. Sci. 62 (2007) 3259–3267, 2007.
[12] J.P. DuPlessis, A. Montillet, J. Comiti, J. Legrand, Pressure drop prediction for flow through high porosity metallic foams, Chem. Eng. Sci. 49 (1994) 3545–3553.
[13] F.C. Buciuman, B. Kraushaar-Czarnetzki, Ceramic foam monoliths as catalyst carriers. 1. Adjustment and description of the morphology, Ind. Eng. Chem. Res. 42 (2003) 1863–1869.
[14] A. Bhattacharya, V.V. Calmidi, et al., Thermophysical properties of high porosity metal foams, Int. J. Heat Mass Transfer 45 (5) (2002) 1017–1031.
[15] J.G. Fourie, J.P. DuPlessis, Pressure drop modelling in cellular metallic foams, Chem. Eng. Sci. 57 (2002) 2781–2789.
[16] E.A. Moreira, J.R. Coury, The influence of structural parameters on the permeability of ceramic foams, Braz. J. Chem. Eng. 21 (01) (2004) 23–33.
[17] M.D.M. Innocentini, Vânia R. Salvini, Alvaro Macebo, Victor C. Pandolfelli, Prediction of ceramic foams permeability using Ergun's equation, Mater. Res. 2 (4) (1999) 283–289.
[18] R.K. Shah, in: S. Kakac, A.E. Bergles, F. Mayinger (Eds.), Heat Exchanger: Thermal–Hydraulic Fundamentals and design, Hemisphere, Washington, DC, 1981.
[19] J.F. Liu, W.T. Wu, W.C. Chiu, W.H. Hsieh, Measurement and correlation of friction characteristic of flow through foam matrixes, Exp. Therm. Fluid Sci 30 (2006) 329–336.
[20] L. Tadrist, M. Miscevic, O. Rahli, F. Topin, About the use of fibrous materials in compact heat exchangers, Exp. Therm. Fluid Sci. 28 (2004) 193–199.
[21] A. Hazen, Some physical properties of sand and gravels with special reference to their use in filtration, Massachusetts State Board of Health, Twenty-fourth Annual Report, 1893, p. 541.
[22] S. Ergun, Fluid flow through packed columns, Chem. Eng. Prog. 48 (2) (1952) 89–94.

[23] I. Iliuta, F. Larachi, Pressure drop and liquid holdup in trickle flow reactors: improved Ergun constants and slip correlations for the slit model, Chem. Eng. Sci. 37 (1998) 4542–4550.
[24] R.A. Holub, M.P. Dudukovic, A phenomenological model for pressure drop, liquid holdup, and flow regime transition in gas–liquid trickle flow, Chem. Eng. Sci. 47 (9–11) (1992) 2343–2348.
[25] F. Topin, J.P. Bonnet, B. Madani, L. Tadrist, Experimental analysis of multiphase flow in metallic foam: flow laws, heat transfer and convective boiling, Adv. Eng. Mater. 8 (2006) 890–899.
[26] P. Khayargoli, V. Loya, L.P. Lefebvre, M. Medraj, The impact of microstructure on the permeability of metal foams, CSME 2004 Forum (2004) 220–228.